Human calprotectin affects the redox speciation of iron

HHS Public Access

Author manuscript

Metallomics. Author manuscript; available in PMC 2018 August 16.

Published in final edited form as:

Metallomics. 2017 August 16; 9(8): 1086–1095. doi:10.1039/c7mt00044h.

Human Calprotectin Affects the Redox Speciation of Iron

Toshiki G. Nakashige and **Elizabeth M. Nolan***

Department of Chemistry, Massachusetts Institute of Technology, Cambridge, MA 02139, USA

Abstract

We report that the metal-sequestering human host-defense protein calprotectin (CP, S100A8/S100A9 oligomer) affects the redox speciation of iron (Fe) in bacterial growth media and buffered aqueous solution. Under aerobic conditions and in the absence of an exogenous reducing agent, CP-Ser (S100A8(C42S)/S100A9(C3S) oligomer) depletes Fe from three different bacterial growth media preparations over a 48-h timeframe (T = 30 °C). The presence of the reducing agent β-mercaptoethanol accelerates this process and allows CP-Ser to deplete Fe over a ≈1-h timeframe. Fe-depletion assays performed with metal-binding-site variants of CP-Ser show that the hexahistidine (His_6) site, which coordinates Fe(II) with high affinity, is required for Fe depletion. An analysis of Fe redox speciation in buffer containing Fe(III) citrate performed under aerobic conditions demonstrates that CP-Ser causes a time-dependent increase in the [Fe(II)]/[Fe(III)] ratio. Taken together, these results indicate that the hexahistidine site of CP stabilizes Fe(II) and thereby shifts the redox equilibrium of Fe to the reduced ferrous state under aerobic conditions. We also report that the presence of bacterial metabolites affects the Fe-depleting activity of CP-Ser. Supplementation of bacterial growth media with an Fe(III)-scavenging siderophore (enterobactin, staphyloferrin B, or desferrioxamine B) attenuates the Fe-depleting activity of CP-Ser. This result indicates that formation of Fe(III)-siderophore complexes blocks CP-mediated reduction of Fe(III) and hence the ability of CP to coordinate Fe(II). In contrast, the presence of pyocyanin (PYO), a redox-cycling phenazine produced by *Pseudomonas aeruginosa* that reduces Fe(III) to Fe(II), accelerates Fe depletion by CP-Ser under aerobic conditions. These findings indicate that the presence of microbial metabolites that contribute to metal homeostasis at the host/pathogen interface can affect the metal-sequestering function of CP.

Graphical Abstract

The metal-chelating host-defense protein human calprotectin promotes the reduction of Fe(III) to Fe(II).

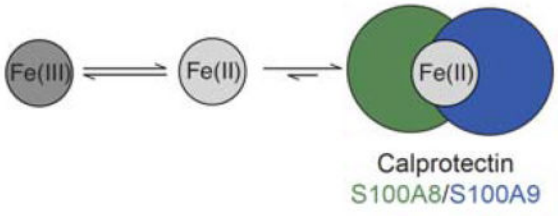

*Corresponding author: lnolan@mit.edu, Phone: 617-452-2495, Fax: 617-324-0505.

Introduction

Iron (Fe) is an essential nutrient for almost all organisms and plays key roles in many life processes.[1] Heme and non-heme iron enzymes utilize this transition metal to carry out a variety of chemical transformations, including reactions involved in primary metabolism, DNA synthesis, defense against oxidative stress, and respiration.[2–4] To maintain the Fe levels required for these important functions, organisms must obtain this transition-metal nutrient from the environment.[5–7] In the context of the host/microbe interaction, the competition between host and microbe for iron is the paradigm for nutritional immunity.[6,8]

Bioavailable iron typically exists in the Fe(III) and Fe(II) oxidation states.[1] The tug-of-war between host and microbe for Fe(III) is accepted to be an important component of innate immunity and microbial pathogenesis.[6,9–11] Humans utilize transferrin (Tf) to scavenge and transport extracellular Fe(III),[7] and deploy the host-defense proteins lactoferrin (Lf)[12,13] and siderocalin (lipocalin-2)[14] at infection sites. These proteins orchestrate an Fe(III)-withholding response to block microbial Fe(III) uptake. Pathogens can evade these host-defense mechanisms by producing and releasing secondary metabolites called siderophores that scavenge Fe(III) from the host,[11,15,16] or by expressing membrane receptors that hijack holo-Tf and -Lf and extract the bound Fe(III) ions.[17–22] In contrast to the wealth of studies examining Fe(III), less is known about the roles of Fe(II) in the host-microbe interaction. Mammals use ferrireductase to reduce extracellular Fe(III) to Fe(II), which is then imported by the transport protein DMT1.[23] Whether additional strategies are employed by the host innate immune system to limit Fe(II) availability requires consideration and exploration.[24] In many bacterial species, the Feo system (*feoABC*) mediates Fe(II) uptake.[25,26] Extracellular Fe(II) can be abundant under oxygen-limiting conditions,[27] and the Feo system has been implicated in the survival and virulence of bacterial pathogens that can inhabit low-oxygen microenvironments in the host, including *Pseudomonas aerugionsa*,[28,29] *Helicobacter pylori*,[30] *Campylobacter jejuni*,[31] *Streptococcus suis*,[32] and the obligate anaerobe *Clostridium perfringens*.[33] In addition to using the Fe(II) permease FeoB for Fe acquisition, the opportunistic human pathogen *Pseudomonas aeruginosa* produces and releases redox-cycling secondary metabolites named phenazines that reduce Fe(III) to Fe(II) in the extracellular environment and therefore proposed to facilitate Fe uptake via FeoB.[28,29] Most recently, a broad-spectrum staphylococcal metallophore named staphylopine was discovered.[34] Staphylopine coordinates divalent first-row transition metals, including Fe(II), and the resulting M(II)-staphylopine complexes are recognized and imported by the Cnt transport system.[34,35]

We recently reported that the metal-sequestering human host-defense protein calprotectin (CP, S100A8/S100A9 oligomer) can bind Fe(II) and block microbial Fe(II) uptake.[24] These observations suggest that CP may contribute to an as-yet unidentified Fe(II)-withholding response in micro-aerobic and anaerobic environments where Fe(II) is available. CP is an abundant metal-scavenging protein that is released from neutrophils during the human innate immune response.[37–43] Each CP heterodimer has four Ca(II)-binding EF-hand domains and two sites, His_3Asp (site 1) and His_6 (site 2), for coordinating divalent transition metal ions (Fig. 1).[36,44,45] Ca(II) binding to the EF-hand domains causes two heterodimers to self-associate and form a heterotetramer that exhibits increased transition-metal affinities

compared to the apo heterodimer.[46,47] In the presence of excess Ca(II), the His_6 site binds Fe(II) as well as Mn(II) and Zn(II) with high affinity (e.g. apparent $K_{d,Fe(II)}$ < 2.2 pM, +Ca).[24] Although site 1 also chelates Fe(II),[48] the affinity of this site for Fe(II) is relatively low, and our prior work indicates that only site 2 contributes to Fe(II) withholding.[24]

We first recognized the ability of CP to coordinate Fe when we conducted metal-depletion assays to determine which metals CP sequestered from bacterial growth medium.[24] In these studies, we used a Tris:TSB medium commonly employed in studies of CP.[45,46,49,50] This medium is often supplemented with a reducing agent, β-mercaptoethanol (BME, ≈3 mM). Tris:TSB prepared in our laboratory typically contains ≈150 nM Mn, ≈3 μM Fe, ≈5 μM Zn and ≈2 mM Ca. During our initial studies, we found that 10.5 μM CP (250 μg/mL) depleted Mn (≈7-fold), Fe (≈23-fold), and Zn (≈60-fold) when the medium was supplemented with BME.[24] These findings contrast an earlier metal-depletion study, performed using aqueous buffer containing divalent cations, which reported that CP only depleted Mn and Zn, and had no effect on Fe.[41] We proposed that BME reduced the Fe(III) in the aerobic Tris:TSB medium to Fe(II), allowing CP to coordinate Fe(II) with high affinity in the presence of ≈2 mM Ca(II).[24] Nevertheless, we also observed that CP depleted Fe from Tris:TSB in the absence of an exogenous reductant, albeit to a lesser degree (≈3-fold). The absence or presence of a reducing agent had negligible effect on the depletion of Mn and Zn.

In this work, we build upon these observations and examine the effect of CP on the speciation of Fe oxidation state in solution. We report a series of metal-depletion experiments that demonstrate (i) slow (≈48 h) Fe depletion by CP in the absence of an exogenous reductant, and (ii) accelerated Fe depletion by CP in the presence of a reducing agent (≈1 h). An analysis of Fe redox speciation reveals that, in the absence of an exogenous reducing agent, CP causes a time-dependent increase the [Fe(II)]/[Fe(III)] ratio in solution. A similar trend is observed with 2,2′-dipyridyl (DP), an Fe(II) chelator that employs neutral nitrogen-donating ligands. Our results indicate that CP causes a shift in the equilibrium between Fe(III) and Fe(II), which allows CP to bind and entrap this metal ion. Moreover, we show that Fe depletion by CP is attenuated by siderophores and enhanced by the presence of a redox-cycling phenazine metabolite under aerobic conditions. These results indicate that microbial metabolites that are released by pathogens during infection can influence the Fe(II)-sequestering ability of CP.

Results

Iron Depletion Under Aerobic Conditions

We first conducted aerobic metal-depletion assays in Tris:TSB in the absence and presence of ≈3 mM BME (Fig. 2, S1–S3). We treated Tris:TSB (±BME) with CP-Ser, ΔHis_3Asp, or ΔHis_4 (10.5 μM, 250 μg/mL; see Table S1 for CP-Ser variant nomenclature) and monitored the metal-depletion profiles of these proteins over a 48-h time period using ICP-MS (Fig. 2, S1–S3). The ΔHis_3Asp and ΔHis_4 variants were used to probe the contributions of each transition-metal-binding site to metal depletion. In the ΔHis_3Asp variant, the four residues that compose the His_3Asp site are mutated to Ala residues (Fig. 1), and the His_6 site is present. In contrast, the ΔHis_4 variant has (A8)His17, (A8)His27, (A9)His91, and (A9)His95 mutated to Ala residues and thus lacks a functional His_6 site. In the presence of BME, CP-

Ser and ΔHis_3Asp readily depleted Fe from the medium within a ≈1-h timeframe. In the absence of BME, Fe depletion by CP-Ser and ΔHis_3Asp occurred, albeit more slowly, with full depletion observed only at the 48-h time point. As expected, no Fe depletion was observed for the ΔHis_4 variant. We also monitored the depletion of other first-row transition metals by ICP-MS and these data are consistent with our prior observations (Fig. S1–S3).[24] For instance, CP-Ser and ΔHis_3Asp completely depleted Mn and Zn from Tris:TSB within 1 h, whereas only Zn depletion was observed for ΔHis_4. As expected, the Mn and Zn depletion profiles were independent of the absence or presence of BME.

To ascertain whether the Fe-depleting behavior of CP-Ser depends on the composition of the growth medium, we repeated this assay using Tris:BHI (≈1.5 μM Fe) and Tris:LB (≈3 μM Fe) mixtures (Fig. S4). Overall, we observed similar trends in the time-dependent depletion of Fe by CP-Ser in these media compared to Tris:TSB when BME is included. However, we note that the magnitude of this "BME effect" varies depending on the medium with Tris:TSB > Tris:BHI ≈ Tris:LB. Indeed, more Fe was depleted from Tris:BHI and Tris:LB at earlier time points compared to Tris:TSB in the absence of the BME supplement. These three media come from different sources (e.g. brain heart infusion for BHI versus soymeal for TSB) and thus have vastly different compositions and, by corollary, metal (and redox) speciation. We reason that the differences in BME-dependent Fe depletion observed likely arise from such inherent differences.

In total, these Fe-depletion assays demonstrate that the presence of a reducing agent enhances the rate of Fe depletion by CP-Ser and ΔHis_3Asp in Tris:TSB and to a lesser degree in the two other media preparations examined in this work. On the basis of the slow Fe depletion observed in the absence of a reducing agent, and a lack of evidence for robust coordination of Fe(III) in prior work, we reasoned that the His_6 site of CP-Ser affects the redox speciation of Fe in the growth media and allows Fe(II) to accumulate under aerobic conditions.

Iron Depletion by CP Under Anaerobic Conditions

We next examined the Fe-depletion profile of CP-Ser under anaerobic conditions. We performed the assay in Tris:TSB (±BME) under a nitrogen atmosphere. Overall, the Fe-depletion profiles under aerobic and anaerobic conditions are similar for the −BME samples (black circles, Fig. 3) and for the +BME samples (red circles, Fig. 3). Under both aerobic and anaerobic conditions, the +BME conditions provide more rapid Fe depletion. Because the same Tris:TSB medium was employed for all samples, this observation likely indicates that deoxygenation of Tris:TSB used for the anaerobic experiments did not have a marked effect on its Fe redox speciation. We note that the data suggest somewhat accelerated depletion of Fe from the −BME medium compared to that observed under aerobic conditions and in the absence of a reducing agent, which is most apparent at the 8-h time point where CP-Ser decreases the Fe content ≈3.1-fold under anaerobic conditions (−BME) compared to ≈1.9 under aerobic conditions (−BME).

Fe(II) Accumulates in the Presence of CP

To further evaluate the Fe-depleting activity of CP and test our hypothesis that CP shifts the redox equilibrium of Fe towards the Fe(II) oxidation state under aerobic conditions, we examined the redox speciation of Fe in aqueous buffer containing 10 μM Fe(III) citrate and either 10.5 μM (250 μg/mL) CP-Ser or the ΔΔ variant, the latter of which has neither the His_3Asp nor the His_6 metal-binding site (Table S1). We quantified Fe(II) and total Fe over time in these solutions by using a ferrozine assay (Fig. 4, S5). Over the course of 72 h, the presence of CP-Ser caused the [Fe(II)]/[Fe(III)] ratio to increase, whereas the presence of ΔΔ had negligible effect on the redox speciation of Fe. These results indicate that CP promotes the reduction of Fe(III) to Fe(II), and are consistent with the notion that Fe depletion results from Fe(II) chelation by CP.

Fe(II) Chelation by a Small Molecule Influences the Iron Redox Speciation

Based on our observations that CP causes an increase in the [Fe(II)]/[Fe(III)] ratio over time, we considered whether this phenomenon occurs with other high-affinity Fe(II) chelators. 2,2′-Dipyridyl (DP) is a neutral bidentate ligand that forms a $[Fe(DP)_3]^{2+}$ complex ($K_{d,Fe(II)}$ = 3.0 × 10^{-18} M).[51,52] Similar to the hexahistidine motif of CP, $[Fe(DP)_3]^{2+}$ exhibits an octahedral site where the Fe(II) ion is coordinated by six neutral nitrogen-donating ligands. Moreover, DP is commonly employed in microbiology experiments to mimic Fe-limited conditions, and the evolution of a pink color in the growth medium is indicative of formation of $[Fe(DP)_3]^{2+}$ (ε_{522} = 8,650 $M^{-1}cm^{-1}$).[51] We added DP to TSB, BHI and LB media, and to buffer containing 10 μM Fe(III) citrate, and monitored formation of $[Fe(DP)_3]^{2+}$ by optical absorbance spectroscopy (Fig. S6). The absorbance at 522 nm increased over the 48-h duration of the experiment. Quantification of total Fe content by ICP-MS (Tables S2) and bound Fe(II) using the reported extinction coefficient of $[Fe(DP)_3]^{2+}$ (Fig. 5) revealed that >40% of the total Fe was bound after a 48-h incubation of each sample. This trend is similar to the time-dependent Fe depletion observed when media was treated with CP-Ser (Fig. 2B).

Siderophores Attenuate Fe Depletion by CP Under Aerobic Conditions

Siderophores are secondary metabolites that coordinate Fe(III) with high affinity.[11] Under conditions of Fe limitation, bacteria biosynthesize and release siderophores to scavenge Fe(III) from the environment. This process is an accepted facet of bacterial pathogenesis, and many siderophores are considered to be virulence factors. Because of the likelihood that siderophores and CP can be co-localized at sites of infection, we monitored Fe depletion from Tris:TSB by CP-Ser in the presence of siderophores (Fig. 6). We supplemented the medium with 3 μM of desferrioxamine B (DFO),[53] enterobactin (Ent),[54] or staphyloferrin B (SB)[55] (Fig. S7). This concentration was chosen because Tris:TSB contains ≈3 μM Fe. The siderophores (400–700 Da) pass through the 10-kDa filter used in this experiment (Fig. 2A); thus, Fe(III)-siderophore complexes that form are present in the CP-treated medium analyzed by ICP-MS. We observed markedly attenuated Fe depletion by CP-Ser in the presence of siderophores (Fig. 6). Negligible Fe depletion occurred when Tris:TSB was supplemented with DFO or Ent, and only ≈30% of Fe was depleted in the presence of SB at the 48-h time point. These results suggest that the (i) Fe predominantly exists as Fe(III) in

Tris:TSB, and (ii) formation of Fe(III)-siderophore complexes in the medium precludes CP from binding Fe under aerobic conditions.

Phenazines Accelerate Fe Depletion by CP

Pyocyanin (PYO) is a redox-cycling phenazine and a conserved virulence factor of *P. aeruginosa*.[56,57] One of the accepted functions of PYO during infection is to reduce Fe(III) to Fe(II) in the extracellular space. This process can cause oxidative stress to the host and other microorganisms by promoting the production of reactive oxygen species through Fenton chemistry.[58] Moreover, it can provide a source of nutrient Fe(II). We observed that supplementation of Tris:TSB with 10 μM PYO resulted in enhanced Fe depletion by CP, comparable to levels observed in the presence of ≈3 mM BME (Fig. 7). This result indicates that redox-cycling metabolites can promote Fe(II) sequestration by CP.

Discussion

In this work, we show that the Fe-depleting activity of CP depends on the redox environment, and that conditions favoring Fe(II) provide relatively rapid depletion of this metal by CP. Moreover, we report that under aerobic conditions and in the absence of a reducing agent, CP causes the [Fe(II)]/[Fe(III)] ratio to increases over time. This observation indicates that Fe(II) coordination by CP causes a shift in the redox speciation of Fe towards Fe(II).

From the standpoints of coordination chemistry and Fe redox speciation, a comparison of CP to well-characterized small molecules that bind Fe with high affinity is informative. The relative affinities of a given ligand for Fe(III) and Fe(II) can be correlated to the Fe(III)/Fe(II) reduction potential for the corresponding complex (Table S3).[59] In general, ligands that employ more electron-donating atoms exhibit higher affinity (lower K_d values) for Fe(III) relative to Fe(II) and lower reduction potential (E^o) values. In an extreme case, the tris-catecholate siderophore Ent with six negatively charged oxygen-donating ligands (Fig. S7) has one of the highest known Fe(III) affinities and a remarkably low reduction potential value ($E^o = -0.75$ V vs. SHE).[60, 61] For ligands that prefer Fe(II) over Fe(III), such as DP and phenanthroline (phen) that employ neutral nitrogen-donating ligands, reduction potentials are relatively high ($E^o = 0.82$ V vs. SHE).[52] The His_6 motif of CP comprises an Fe(II) coordination environment similar to the primary coordination spheres of $[Fe(DP)_3]^{2+}$ and $[Fe(phen)_3]^{2+}$ in that six nitrogen-donors bind the metal ion, and our work demonstrates that this biological site stabilizes the formation of the Fe(II) ion.

From the standpoint of how CP contributes to the host/microbe interaction, our studies suggest microbial metabolites that are involved in virulence and Fe homeostasis can modulate the battle between CP and microbes for nutrient metals. In particular, our work indicates that metallophores and redox-cycling metabolites, which contribute to metal speciation at infection sites, require consideration in mechanistic studies of metal-withholding by CP.

Siderophores are important Fe(III)-scavenging secondary metabolites utilized by many bacterial pathogens to acquire this metal nutrient from the host, and these molecules are

considered to be virulence factors.[11] The ability of siderophores to prevent Fe depletion by CP likely points to an unappreciated facet of the tug-of-war for nutrient Fe between host proteins and microbial Fe acquisition systems. Additionally, phenazines are virulence factors of *P. aeruginosa* that reduce Fe(III) to Fe(II) in the extracellular space. We found that PYO enhances the ability of CP to coordinate Fe(II) under aerobic conditions, and suggests that phenazines and other redox-active metabolites may influence what metals are sequestered by CP at biological sites. The observations from this work allow us to hypothesize that CP may contribute to iron homeostasis in reducing or low-oxygen environments that favor Fe(II), and under conditions where microbial siderophore production is low and microbial Fe(II) uptake machinery is employed. Along these lines, CP was identified early on as the "cystic fibrosis antigen."[62] *P. aeruginosa* is an iron-centric Gram-negative bacterium that colonizes the lungs of cystic fibrosis patients and causes debilitating chronic infections.[28,29] A large body of evidence demonstrates that: (i) the infected regions of the cystic fibrosis lung are reducing and hypoxic;[63,64] (ii) Fe(II) is an abundant and important iron source for *P. aeruginosa* in this environment;[27] and (iii) phenazine concentrations and the [Fe(II)]/[Fe(III)] ratio in cystic fibrosis sputum increase as lung function declines.[65] Taken together, the chemical and redox environment of the infected CF lung favors Fe(II) and may also promote Fe(II) chelation by CP. We reason that evaluating the interplay between *P. aeruginosa* and CP in the context of chronic CF lung disease may reveal new insight into the human metal-withholding response as well as the homeostasis of iron and other transition metal nutrients at the host/pathogen interface.

Conclusion

CP is an important innate immune protein that contributes to the first line of defense against invading microbes by sequestering nutrient transition metals. This work shows that CP can influence the oxidation state of Fe in solution and stabilizes Fe(II) under aerobic conditions. It is possible that the ability of CP to influence Fe redox speciation plays a physiological role in Fe homeostasis at the host-pathogen interface. These exploratory studies provide a foundation for future investigations aimed at understanding the interplay between CP, microbes, and Fe.

Experimental

Materials and General Methods

All chemicals were obtained from commercial suppliers and used as received unless otherwise noted. Milli-Q water (18.2 MΩ•cm, 0.22-μm filter) was used for all aqueous solutions and media. Buffers were prepared with Ultrol grade HEPES (Calbiochem), TraceSELECT NaCl (Sigma), and TraceSELECT NaOH (Sigma) in acid-washed volumetric glassware, using disposable plastic spatulas. Metal stock solutions were prepared in acid-washed volumetric glassware. Ca(II) stock solutions (1.0 M) were prepared with 99.99% anhydrous $CaCl_2$ (Sigma) in water. Fe(III) stock solutions (100 mM) were prepared by dissolving 99.99% $FeCl_3$ (Sigma) in 0.1 M HCl (diluted from a concentrated solution, trace metals basis, Sigma), and stock solutions of Fe(III) citrate (50 mM) were prepared by preparing a 1:1 (v/v) mixture of the $FeCl_3$ stock solution and a 100-mM solution of sodium

citrate tribasic dehydrate (≥99.5%, Sigma). Fe(II) stock solutions (100 mM) were prepared by dissolving 99.99% $(NH_4)_2Fe(SO_4)_2•6H_2O$ (Sigma) into deoxygenated water in a nitrogen glove box (Vacuum Atmospheres Company OMNI-LAB). All Fe(II) solutions were handled anaerobically. Working metal stock solutions prepared by serial dilution immediately before each experiment and stored in polypropylene containers.

All proteins were overexpressed and purified as described previously.[46,50] Native CP was purified in the presence of 5 mM 1,4-dithiothreitol (DTT, OmniPur, Calbiochem). CP variants are based on CP-Ser, the heterooligomer of S100A8(C3S) and S100A9(C42S) (Table S1). Tryptic soy broth (TSB), blood-heart infusion (BHI) medium, and Luria-Bertani (LB) broth were prepared by dissolving commercially available powder (BD) in water and autoclaving in glass bottles. Tris buffer (50 mL) containing 20 mM Tris, 100 mM NaCl, 2 mM $CaCl_2$, pH 7.5 in the absence and presence of 5 mM BME (Alfa Aesar) was prepared by diluting stock solutions of 1.0 M Tris-HCl (molecular biology grade, Alfa Aesar), 1.0 M NaCl (molecular biology grade, Sigma), and 1.0 M $CaCl_2$. This buffer was sterilized by syringe filtration (0.22 μm). Mixtures of Tris:TSB ±BME, Tris:BHI ±BME, and Tris:LB ±BME were routinely prepared by Mixing a 62:38 (v:v) ratio of Tris buffer and sterile medium in sterile 50-mL Falcon tubes. Amicon spin filters (10K MWCO, 4 mL or 15 mL, Millipore) were used to remove protein from media samples.

Optical Absorption Spectroscopy

Absorbance measurements were conducted using a Beckman Coulter DU 800 spectrophotometer with a Peltier temperature controller set to 25 ºC. A BioTek Synergy HT plate reader and a Take3 plate were routinely used to determine CP concentration (ε_{280} = 18,450 $M^{-1}cm^{-1}$, calculated using the ExPASy ProtParam online tool from SIB Swiss Institute of Bioinformatics). Optical density (OD_{600}) measurements for bacterial cultures grown in flat-bottom 96-well plates (Corning, Inc.) were conducted by using the plate reader.

Inductively Coupled Plasma-Mass Spectrometry (ICP-MS)

Elemental analysis was conducted using an Agilent 7900 ICP-MS system in helium mode outfitted with an integrated autosampler housed in the Center for Environmental Health Sciences (CEHS) Core Facility at MIT. The instrument was calibrated using standards prepared by serially diluting an Environmental Calibration Standard solution (Agilent) into 3% nitric acid, which was prepared from concentrated HNO_3 (trace metals basis, Sigma) diluted in Milli-Q water. The concentrations of Mg, Ca, Mn, Fe, Co, Ni, Cu, and Zn were quantified, and 1 ppb terbium (Agilent) was used as an internal standard. Samples were generally prepared in 15-mL Falcon tubes, and 2-mL samples were transferred to acid-washed plastic ICP-MS vials and analyzed.

Medium Metal-Depletion Assays

The metal content of CP-treated medium was measured over time following a modified protocol.[24] Protein samples were buffer exchanged into Tris buffer (20 mM Tris, 100 mM NaCl, 3 mM $CaCl_2$ pH 7.5) using 0.5-mL 10K MWCO Amicon spin filters (Millipore). For a standard assay, 20 mL of medium were incubated with 10.5 μM CP in 50-mL Falcon tubes

at 30 ºC, 150 rpm. At time points t = 2, 4, 8, 24, and 48 h, ≈2.5 mL of medium were transferred to a spin filter and centrifuged (15 min, 3750 rpm, 4 ºC). The flow through or "CP-treated medium" (2 mL) was transferred to a 15-mL Falcon tube, to which 100 μL of concentrated HNO_3 and 1 ppb Tb (40 μL of 50 ppb Tb) were added. The samples were analyzed by ICP-MS. To measure the metal content before CP treatment (t = 0 h time point), an untreated medium sample was run for every experiment.

To determine the effect of siderophores on metal depletion, siderophore (3 μM) was preincubated in Tris:TSB −BME prior to the CP-treatment protocol described above. Desferrioxamine B (DFOB) was purchased from Sigma, and a 100-mM stock solution was prepared in water. Enterobactin (Ent) and staphyloferrin B (SB) were synthesized as previously described,[55,66] and stock solutions (≈20 mM) were prepared in anhydrous dimethyl sulfoxide (DMSO, Sigma). For metal-depletion samples containing pyocyanin (PYO), 10 μM PYO (≥98%, Sigma, 10 mM stock solution in DMSO) was added to Tris:TSB −BME prior to the CP-treatment protocol described above. PYO from a 1-mM stock solution prepared in DMSO. Samples containing PYO or SB were stored and incubated in the dark.

Metal-depletion assays were also performed under anaerobic conditions in a glove box. The inside of the glove box was sterilized by wiping surfaces with isopropanol. For these experiments, TSB was prepared in the glove box by dissolving powder into deoxygenated water and sterilized by syringe filtration (0.22 μm). The Tris:TSB ±BME solution was prepared by mixing filter-sterilized deoxygenated Tris buffer with TSB. Anaerobic samples were stored in 16 × 125 mm glass anaerobic Hungate culture tubes with a butyl stoppers and screw caps (Chemglass Life Sciences) and were incubated at 30 ºC, 150 rpm outside of the glove box. At each time point, the tubes were transferred into the glove box and an aliquot of sample was removed from each tube and transferred into a spin filter. For all assays, three independent trials were conducted, and the mean and SDM are reported (n = 3).

Fe Speciation Assay with Ferrozine

Before each trial, solutions of sodium ascorbate (Asc, ≥99.0%, Sigma; 1.5 mM in 0.2 M HCl), trichloroacetic acid (TCA, ≥99.5%, Sigma; 0.4 M in water), and ammonium acetate (trace metals basis, Sigma; 1.3 M in water) were prepared in 50-mL Falcon tubes. Stock solutions (100 mM) of ferrozine (3-(2-pyridyl)-5,6-diphenyl-1,2,4-triazine-p,p'-disulfonic acid monosodium salt hydrate, 97%, Sigma) were prepared in water, partitioned into ≈1-mL aliquots in microcentrifuge tubes, and stored at −80 ºC until use. Working solutions of 6.17 mM ferrozine were prepared by diluting an aliquot of the stock solution into 0.1 M HCl.

Solutions (5 mL) of 10 μM Fe(III) citrate were prepared in 75 mM HEPES, 100 mM NaCl, 2 mM $CaCl_2$, pH 7.0 and stored in 15-mL polypropylene culture tubes. To each solution, 10.5 μM (250 μg/mL) CP-Ser or ΔΔ was added. The samples were incubated at 30 ºC, 150 rpm. At time points t = 0, 24, 48, and 72 h, two 200-μL aliquots of each solution were transferred from the culture tube to two microcentrifuge tubes. To quantify the levels of Fe(II) and total Fe in solution, a modified ferrozine assay was conducted.[67] For each pair of samples, either 200 μL of 0.2 M HCl (to quantify Fe(II)) or 200 μL of 1.5 mM Asc (to quantify total Fe) were added, and then 200 μL of TCA were added. The resulting sample was vortexed for 10

s, heated to 95 ºC for 5 min, and centrifuged (13,000 rpm, 5 min, 4 ºC). The supernatant (300 μL) was transferred to a new microcentrifuge tube, and ammonium acetate (1.3 mM, 400 μL) and ferrozine (6.17 mM, 100 μL) were added. The sample was vortexed and a 500-μL aliquot was transferred to a disposable cuvette. The optical absorption spectrum (400–800 nm) was collected, and Fe was quantified using the extinction coefficient of the Fe-ferrozine complex (ε_{562} = 27,900 M^{-1} cm^{-1}).[67] Standards (0–32 μM Fe(III) citrate) were also prepared and analyzed as above, and a standard curve was used to determine Fe concentrations of the samples. The Fe(III) concentration for each sample was determined by subtracting the Fe(II) concentration (−Asc) from the total Fe concentration (+Asc). Six independent trials were conducted, and the mean and SDM are reported (n = 6).

Treatment of Bacterial Growth Medium with 2,2′-Dipyridyl

Stock solutions of 100-mM 2,2′-dipyridyl (DP, ≥99%, Sigma, 100 mM in DMSO) were prepared, partitioned into ≈200-μL aliquots in microcentrifuge tubes, and stored at −80 ºC until use. In 15-mL culture tubes, 5-mL solutions of TSB, BHI, LB, and 10 μM Fe(III) citrate in buffer (75 mM HEPES, 100 mM NaCl, 2 mM $CaCl_2$, pH 7.0) were prepared. For the t = 0 h time point, the absorbance spectrum (400–800 nm) for each sample was recorded. DP (1 mM) was then added, and the samples were incubated at 30 ºC, 150 rpm. At t = 2, 4, 8, 24, and 48 h, the absorbance spectra were recorded. Six independent trials were conducted, and the mean and SDM are reported (n = 6). For quantifying Fe(II) at each time point, the reported extinction coefficient of DP (ε_{522} = 8,650 $M^{-1}cm^{-1}$, confirmed for the buffer conditions used in this work).[51] Total metal content of the media was quantified by ICP-MS. For a 2-mL sample of medium, 100 μL of concentrated HNO_3 and 40 μL of 50 ppb Tb were added, and the resulting mixture was analyzed.

Supplementary Material

Refer to Web version on PubMed Central for supplementary material.

Acknowledgments

We acknowledge Dr. Phoom Chairatana for synthesizing enterobactin and Mr. Anmol Gulati for synthesizing staphyloferrin B. We thank Ms. Anna Wuttig and Dr. Timothy C. Johnstone for providing helpful discussions. We gratefully acknowledge the MIT Center for Environmental Health Sciences (NIH P30-ES002109), the Sloan Foundation, the MIT Research Support Committee (Wade Award), and the National Science Foundation Graduate Research Fellowship (NSF) for financial support. *E. coli* K-12 was obtained from the Keio Collection,[68] and *P. aeruginosa* PAO1 was obtained from the Seattle Collection.[695,70] We acknowledge the Network on Antimicrobial Resistance in *Staphylococcus aureus* (NARSA) for providing the *S. aureus* USA300 JE2 strain of the Nebraska Transposon Mutant Library (NTML) that is supported by NIH NIAID grant HHSN272200700055C.[71]

References

1. Frey PA, Reed GH. The ubiquity of iron. ACS Chem Biol. 2012; 7:1477–1481. [PubMed: 22845493]
2. Babcock GT. How oxygen is activated and reduced in respiration. Proc Natl Acad Sci USA. 1999; 96:12971–12973. [PubMed: 10557256]
3. Stubbe J, Nocera DG, Yee CS, Chang MCY. Radical initiation in the class I ribonucleotide reductase: Long-range proton-coupled electron transfer? Chem Rev. 2003; 103:2167–2202. [PubMed: 12797828]

4. Lah MS, Dixon MM, Pattridge KA, Stallings WC, Fee JA, Ludwig ML. Structure-function in *Escherichia coli* iron superoxide dismutase: Comparisons with the manganese enzyme from *Thermus thermophilus*. Biochemistry. 1995; 34:1646–1660. [PubMed: 7849024]
5. De Domenico I, McVey Ward D, Kaplan J. Regulation of iron acquisition and storage: consequences for iron-linked disorders. Nat Rev Mol Cell Biol. 2008; 9:72–81. [PubMed: 17987043]
6. Cassat JE, Skaar EP. Iron in infection and immunity. Cell Host Microbe. 2013; 13:509–519. [PubMed: 23684303]
7. Pantopoulos K, Porwal SK, Tartakoff A, Devireddy L. Mechanisms of mammalian iron homeostasis. Biochemistry. 2012; 51:5705–5724. [PubMed: 22703180]
8. Weinberg ED. Nutritional immunity: Host's attempt to withhold iron from microbial invaders. J Am Med Assoc. 1975; 231:39–41.
9. Braun V. Iron uptake mechanisms and their regulation in pathogenic bacteria. Int J Med Microbiol. 2001; 291:67–79. [PubMed: 11437341]
10. Fischbach MA, Lin HN, Liu DR, Walsh CT. How pathogenic bacteria evade mammalian sabotage in the battle for iron. Nat Chem Biol. 2006; 2:132–138. [PubMed: 16485005]
11. Miethke M, Marahiel MA. Siderophore-based iron acquisition and pathogen control. Microbiol Mol Biol Rev. 2007; 71:413–451. [PubMed: 17804665]
12. Vogel HJ. Lactoferrin, a bird's eye view INTRODUCTION. Biochem Cell Biol. 2012; 90:233–244. [PubMed: 22540735]
13. Sanchez L, Calvo M, Brock JH. Biological role of lactoferrin. Arch Dis Child. 1992; 67:657–661. [PubMed: 1599309]
14. Flo TH, Smith KD, Sato S, Rodriguez DJ, Holmes MA, Strong RK, Akira S, Aderem A. Lipocalin 2 mediates an innate immune response to bacterial infection by sequestrating iron. Nature. 2004; 432:917–921. [PubMed: 15531878]
15. Bagg A, Neilands JB. Molecular mechanism of regulation of siderophore-mediated iron assimilation. Microbiol Rev. 1987; 51:509–518. [PubMed: 2963952]
16. Fischbach MA, Lin H, Zhou L, Yu Y, Abergel RJ, Liu DR, Raymond KN, Wanner BL, Strong RK, Walsh CT, Aderem A, Smith KD. The pathogen-associated *iroA* gene cluster mediates bacterial evasion of lipocalin 2. Proc Natl Acad Sci U S A. 2006; 103:16502–16507. [PubMed: 17060628]
17. Mickelsen PA, Sparling PF. Ability of Neisseria gonorrhoeae, Neisseria meningitidis, and commensal *Neisseria* species to obtain iron from transferrin and iron compounds. Infect Immun. 1981; 33:555–564. [PubMed: 6792081]
18. Mickelsen PA, Blackman E, Sparling PF. Ability of Neisseria gonorrhoeae, Neisseria meningitidis, and commensal *Neisseria s*pecies to obtain iron from lactoferrin. Infect Immun. 1982; 35:915–920. [PubMed: 6121757]
19. Noinaj N, Easley NC, Oke M, Mizuno N, Gumbart J, Boura E, Steere AN, Zak O, Aisen P, Tajkhorshid E, Evans RW, Gorringe AR, Mason AB, Steven AC, Buchanan SK. Structural basis for iron piracy by pathogenic *Neisseria*. Nature. 2012; 483:53–58. [PubMed: 22327295]
20. Calmettes C, Alcantara J, Yu RH, Schryvers AB, Moraes TF. The structural basis of transferrin sequestration by transferrin-binding protein B. Nat Struct Mol Biol. 2012; 19:358–360. [PubMed: 22343719]
21. Noinaj N, Cornelissen CN, Buchanan SK. Structural insight into the lactoferrin receptors from pathogenic *Neisseria*. J Struct Biol. 2013; 184:83–92. [PubMed: 23462098]
22. Morgenthau A, Pogoutse A, Adamiak P, Moraes TF, Schryvers AB. Bacterial receptors for host transferrin and lactoferrin: molecular mechanisms and role in host-microbe interactions. Future Microbiol. 2013; 8:1575–1585. [PubMed: 24266357]
23. Hentze MW, Muckenthaler MU, Galy B, Camaschella C. Two to tango: Regulation of mammalian iron metabolism. Cell. 2010; 142:24–38. [PubMed: 20603012]
24. Nakashige TG, Zhang B, Krebs C, Nolan EM. Human calprotectin is an iron-sequestering host-defense protein. Nat Chem Biol. 2015; 11:765–771. [PubMed: 26302479]
25. Lau CKY, Krewulak KD, Vogel HJ. Bacterial ferrous iron transport: the Feo system. FEMS Microbiol Rev. 2016; 40:273–298. [PubMed: 26684538]

26. Stojiljkovic I, Cobeljic M, Hantke K. *Escherichia coli* K-12 ferrous iron uptake mutants are impaired in their ability to colonize the mouse intestine. FEMS Microbiol Lett. 1993; 108:111–115. [PubMed: 8472918]
27. Hunter RC, Asfour F, Dingemans J, Osuna BL, Samad T, Malfroot A, Cornelis P, Newman DK. Ferrous iron is a significant component of bioavailable iron in cystic fibrosis airways. mBio. 2013; 4:e00557–00513.
28. Konings AF, Martin LW, Sharples KJ, Roddam LF, Latham R, Reid DW, Lamont IL. *Pseudomonas aeruginosa* uses multiple pathways to acquire iron during chronic infection in cystic fibrosis lungs. Infect Immun. 2013; 81:2697–2704. [PubMed: 23690396]
29. Cornelis P, Dingemans J. *Pseudomonas aeruginosa* adapts its iron uptake strategies in function of the type of infections. Front Cell Infect Microbiol. 2015
30. Velayudhan J, Hughes NJ, McColm AA, Bagshaw J, Clayton CL, Andrews SC, Kelly DJ. Iron acquisition and virulence in Helicobacter pylori: a major role for FeoB, a high-affinity ferrous iron transporter. Mol Microbiol. 2000; 37:274–286. [PubMed: 10931324]
31. Naikare H, Palyada K, Panciera R, Marlow D, Stintzi A. Major role for FeoB in Campylobacter jejuni ferrous iron acquisition, gut colonization, and intracellular survival. Infect Immun. 2006; 74:5433–5444. [PubMed: 16988218]
32. Aranda J, Cortes P, Garrido ME, Fittipaldi N, Llagostera M, Gottschalk M, Barbe J. Contribution of the FeoB transporter to *Streptococcus suis* virulence. Int Microbiol. 2009; 12:137–143. [PubMed: 19784934]
33. Awad MM, Cheung JK, Tan JE, McEwan AG, Lyras D, Rood JI. Functional analysis of an feoB mutant in *Clostridium perfringens* strain 13. Anaerobe. 2016; 41:10–17. [PubMed: 27178230]
34. Ghssein G, Brutesco C, Ouerdane L, Fojcik C, Izaute A, Wang S, Hajjar C, Lobinski R, Lemaire D, Richaud P, Voulhoux R, Espaillat A, Cava F, Pignol D, Borezée-Durant E, Arnoux P. Biosynthesis of a broad-spectrum nicotianamine-like metallophore in *Staphylococcus aureus*. Science. 2016; 352:1105–1109. [PubMed: 27230378]
35. Remy L, Carrière M, Derré-Bobillot A, Martini C, Sanguinetti M, Borezée-Durant E. The *Staphylococcus aureus* Opp1 ABC transporter imports nickel and cobalt in zinc-depleted conditions and contributes to virulence. Mol Microbiol. 2013; 87:730–743. [PubMed: 23279021]
36. Gagnon DM, Brophy MB, Bowman SE, Stich TA, Drennan CL, Britt RD, Nolan EM. Manganese binding properties of human calprotectin under conditions of high and low calcium: X-ray crystallographic and advanced electron paramagnetic resonance spectroscopic analysis. J Am Chem Soc. 2015; 137:3004–3016. [PubMed: 25597447]
37. Kehl-Fie TE, Skaar EP. Nutritional immunity beyond iron: A role for manganese and zinc. Curr Opin Chem Biol. 2010; 14:218–224. [PubMed: 20015678]
38. Hood MI, Skaar EP. Nutritional immunity: Transition metals at the pathogen–host interface. Nat Rev Microbiol. 2012; 10:525–537. [PubMed: 22796883]
39. Diaz-Ochoa VE, Jellbauer S, Klaus S, Raffatellu M. Transition metal ions at the crossroads of mucosal immunity and microbial pathogenesis. Front Cell Infect Microbiol. 2014; 4:2. [PubMed: 24478990]
40. Sohnle PG, Collins-Lech C, Wiessner JH. The zinc-reversible antimicrobial activity of neutrophil lysates and abscess fluid supernatants. J Infect Dis. 1991; 164:137–142. [PubMed: 2056200]
41. Corbin BD, Seeley EH, Raab A, Feldmann J, Miller MR, Torres VJ, Anderson KL, Dattilo BM, Dunman PM, Gerads R, Caprioli RM, Nacken W, Chazin WJ, Skaar EP. Metal chelation and inhibition of bacterial growth in tissue abscesses. Science. 2008; 319:962–965. [PubMed: 18276893]
42. Clohessy PA, Golden BE. Calprotectin-mediated zinc chelation as a biostatic mechanism in host defence. Scand J Immunol. 1995; 42:551–556. [PubMed: 7481561]
43. Johne B, Fagerhol MK, Lyberg T, Prydz H, Brandtzaeg P, Naess-Andresen CF, Dale I. Functional and clinical aspects of the myelomonocyte protein calprotectin. J Clin Pathol: Mol Pathol. 1997; 50:113–123.
44. Korndörfer IP, Brueckner F, Skerra A. The crystal structure of the human $(S100A8/S100A9)_2$ heterotetramer, calprotectin, illustrates how conformational changes of interacting α-helices can

determine specific association of two EF-hand proteins. J Mol Biol. 2007; 370:887–898. [PubMed: 17553524]

45. Damo SM, Kehl-Fie TE, Sugitani N, Holt ME, Rathi S, Murphy WJ, Zhang Y, Betz C, Hench L, Fritz G, Skaar EP, Chazin WJ. Molecular basis for manganese sequestration by calprotectin and roles in the innate immune response to invading bacterial pathogens. Proc Natl Acad Sci USA. 2013; 110:3841–3846. [PubMed: 23431180]
46. Brophy MB, Hayden JA, Nolan EM. Calcium ion gradients modulate the zinc affinity and antibacterial activity of human calprotectin. J Am Chem Soc. 2012; 134:18089–18100. [PubMed: 23082970]
47. Hayden JA, Brophy MB, Cunden LS, Nolan EM. High-affinity manganese coordination by human calprotectin is calcium-dependent and requires the histidine-rich site formed at the dimer interface. J Am Chem Soc. 2013; 135:775–787. [PubMed: 23276281]
48. Baker TM, Nakashige TG, Nolan EM, Neidig ML. Magnetic circular dichroism studies of iron(II) binding to human calprotectin. Chem Sci. 2017; 8:1369–1377. [PubMed: 28451278]
49. Kehl-Fie TE, Chitayat S, Hood MI, Damo S, Restrepo N, Garcia C, Munro Kim A, Chazin Walter J, Skaar Eric P. Nutrient metal sequestration by calprotectin inhibits bacterial superoxide defense, enhancing neutrophil killing of *Staphylococcus aureus*. Cell Host Microbe. 2011; 10:158–164. [PubMed: 21843872]
50. Brophy MB, Nakashige TG, Gaillard A, Nolan EM. Contributions of the S100A9 C-terminal tail to high-affinity Mn(II) chelation by the host-defense protein human calprotectin. J Am Chem Soc. 2013; 135:17804–17817. [PubMed: 24245608]
51. Hazra DK, Lahiri SC. The dissociation constants of 2,2′-bipyridine and its iron(II) complex in water-methanol mixtures. Anal Chim Acta. 1975; 79:335–340.
52. Smith, RM., Martell, AE. Critical Stability Constants Volume 2: Amines. Plenum Press; New York: 1975.
53. Farkas E, Enyedy ÉA, Csóka H. A comparison between the chelating properties of some dihydroxamic acids, desferrioxamine B and acetohydroxamic acid. Polyhedron. 1999; 18:2391–2398.
54. Loomis LD, Raymond KN. Solution equilibria of enterobactin and metal-enterobactin complexes. Inorg Chem. 1991; 30:906–911.
55. Madsen JLH, Johnstone TC, Nolan EM. Chemical synthesis of staphyloferrin B affords insight into the molecular structure, iron chelation, and biological activity of a polycarboxylate siderophore deployed by the human pathogen *Staphylococcus aureus*. J Am Chem Soc. 2015; 137:9117–9127. [PubMed: 26030732]
56. Lau GW, Hassett DJ, Ran H, Kong F. The role of pyocyanin in *Pseudomonas aeruginosa* infection. Trends Mol Med. 2004; 10:599–606. [PubMed: 15567330]
57. Price-Whelan A, Dietrich LE, Newman DK. Rethinking ‘secondary’ metabolism: physiological roles for phenazine antibiotics. Nat Chem Biol. 2006; 2:71–78. [PubMed: 16421586]
58. Hassan HM, Fridovich I. Mechanism of the antibiotic action pyocyanine. J Bacteriol. 1980; 141:156–163. [PubMed: 6243619]
59. Rizvi MA, Mane M, Khuroo MA, Peerzada GM. Computational survey of ligand properties on iron(III)–iron(II) redox potential: exploring natural attenuation of nitroaromatic compounds. Monatsh Chem. 2016; doi: 10.1007/s00706-016-1813-8
60. Harris WR, Carrano CJ, Cooper SR, Sofen SR, Avdeef AE, McArdle JV, Raymond KN. Coordination chemistry of microbial iron transport compounds. 19. Stability constants and electrochemical behavior of ferric enterobactin and model complexes. J Am Chem Soc. 1979; 101:6097–6104.
61. Lee CW, Ecker DJ, Raymond KN. The pH-dependent reduction of ferric enterobactin probed by electrochemical methods and its implications for microbial iron transport. J Am Chem Soc. 1985; 107:6920–6923.
62. Dorin JR, Novak M, Hill RE, Brock DJ, Secher DS, van Heyningen V. A clue to the basic defect in cystic fibrosis from cloning the CF antigen gene. Nature. 1987; 326:614–617.

63. Cowley ES, Koph SH, LaRiviere A, Ziebis W, Newman DK. Pediatric cystic fibrosis sputum can be chemically dynamics, anoxic, and extremely reduced due to hydrogen sulfide formation. mBio. 2015; 6:e00767–15. [PubMed: 26220964]

64. Worlitzsch D, Tarran R, Ulrich M, Schwab U, Cekici A, Meyer KC, Birrer P, Bellon G, Berger J, Weiss T, Botzenhart K, Yankaskas JR, Randell S, Boucher RC, Doring G. Effects of reduced mucus oxygen concentration in airway *Pseudomonas* infections of cystic fibrosis patients. J Clin Invest. 2002; 109:317–325. [PubMed: 11827991]

65. Hunter RC, Klepac-Ceraj V, Lorenzi MM, Grotzinger H, Martin TR, Newman DK. Phenazine content in the cystic fibrosis respiratory tract negatively correlates with lung function and microbial complexity. Am J Respir Cell Mol Biol. 2012; 47:738–745. [PubMed: 22865623]

66. Zheng T, Bullock JL, Nolan EM. Siderophore-mediated cargo delivery to the cytoplasm of *Escherichia coli* and *Pseudomonas aeruginosa*: Syntheses of monofunctionalized enterobactin scaffolds and evaluation of enterobactin–cargo conjugate uptake. J Am Chem Soc. 2012; 134:18388–18400. [PubMed: 23098193]

67. Stookey LL. Ferrozine—a new spectrophotometric reagent for iron. Anal Chem. 1970; 42:779–781.

68. Baba T, Ara T, Hasegawa M, Takai Y, Okumura Y, Baba M, Datsenko KA, Tomita M, Wanner BL, Mori H. Construction of Escherichia coli K-12 in-frame, single-gene knockout mutants: the Keio collection. Mol Syst Biol. 2006; 2:2006.0008.

69. Jacobs MA, Alwood A, Thaipisuttikul I, Spencer D, Haugen E, Ernst S, Will O, Kaul R, Raymond C, Levy R, Chun-Rong L, Guenthner D, Bovee D, Olson MV, Manoil C. Comprehensive transposon mutant library of *Pseudomonas aeruginosa*. Proc Natl Acad Sci USA. 2003; 100:14339–14344. [PubMed: 14617778]

70. Held K, Ramage E, Jacobs M, Gallagher L, Manoil C. Sequence-verified two-allele transposon mutant library for *Pseudomonas aeruginosa* PAO1. J Bacteriol. 2012; 194:6387–6389. [PubMed: 22984262]

71. Bose JL, Fey PD, Bayles KW. Genetic tools to enhance the study of gene function and regulation in *Staphylococcus aureus*. Appl Environ Microbiol. 2013; 79:2218–2224. [PubMed: 23354696]

Significance

Calprotectin contributes to the metal-withholding innate immune response by limiting nutrient transition metal availability to microbes. We show that (i) the hexahistidine site of calprotectin, which binds Fe(II) with high affinity, contributes to a shift in redox equilibrium from Fe(III) to Fe(II) in solution, and (ii) secondary metabolites that are released by pathogens can attenuate or promote Fe(II) sequestration by calprotectin. This work indicates that the ability of calprotectin to modulate Fe redox speciation may influence Fe availability at biological sites. It highlights that the interplay of calprotectin, microbial metabolites, and metals may have consequences for the metal-withholding response and microbial pathogenesis.

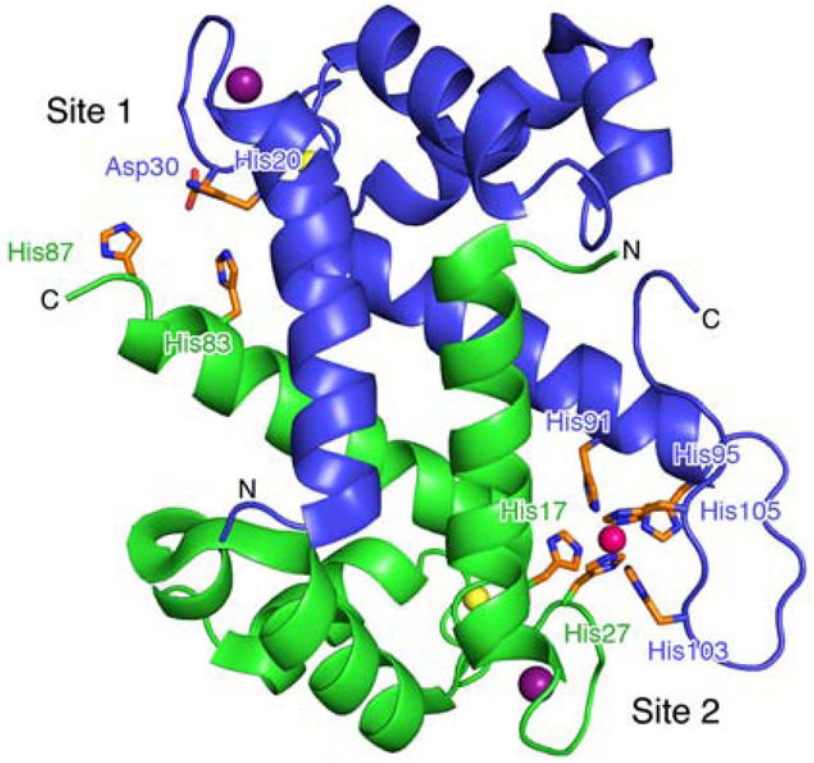

Fig. 1.

The CP heterodimer has two sites that bind transition metals (PDB: 4XJK).[36] Site 1 is the His_3Asp motif, comprising residues His83 and His87 of S100A8 (green, α) and His20 and Asp30 of S100A9 (blue, β). Site 2 is the His_6 motif, comprising residues His17 and His27 of S100A8 and His91, His95, His103, and His105 of S100A9. The αβ heterodimer model of the crystal structure of CP bound to Mn(II) (pink sphere) at site 2, Ca(II) (yellow spheres) at the C-terminal EF-hand domains, and Na(I) (dark purple spheres) at the N-terminal EF-hand domains is shown. The N- and C-termini of each subunit are labeled.

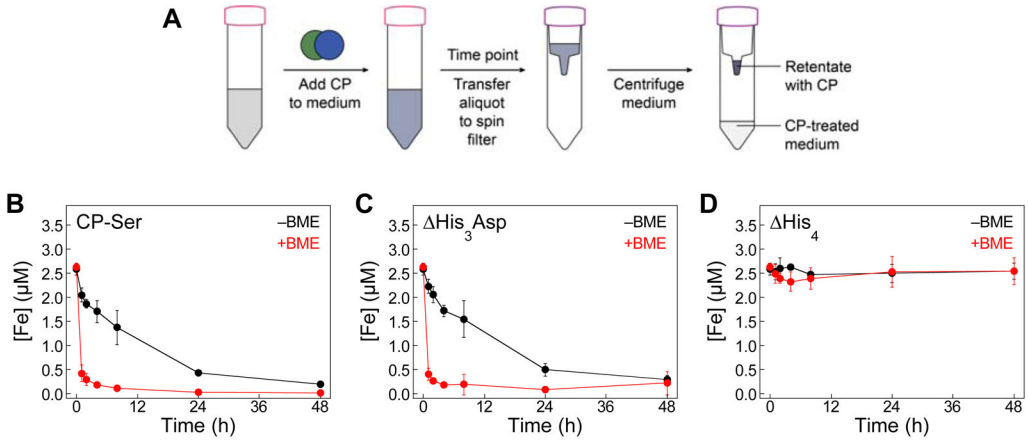

Fig. 2.

Iron depletion by CP-Ser, ΔHis_3Asp and ΔHis_4 under aerobic conditions. (A) Cartoon schematic of the metal-depletion assay. Bacterial growth medium was treated with 10.5 μM CP (250 μg/mL) and incubated at 30 ºC, 150 rpm. At a given time point, an aliquot of medium was transferred to a spin filter. Following centrifugation to remove CP, and the CP-treated medium was analyzed by ICP-MS. (B–D) Tris:TSB treated CP-Ser, ΔHis_3Asp, or ΔHis_4 in the absence (black) or presence (red) of ≈3 mM BME. The metal content in the CP-treated medium was analyzed by ICP-MS at t = 0, 1, 2, 4, 8, 24, and 48 h. The mean and SDM are reported (n = 3). Data for other transition metals are presented in Fig. S1.

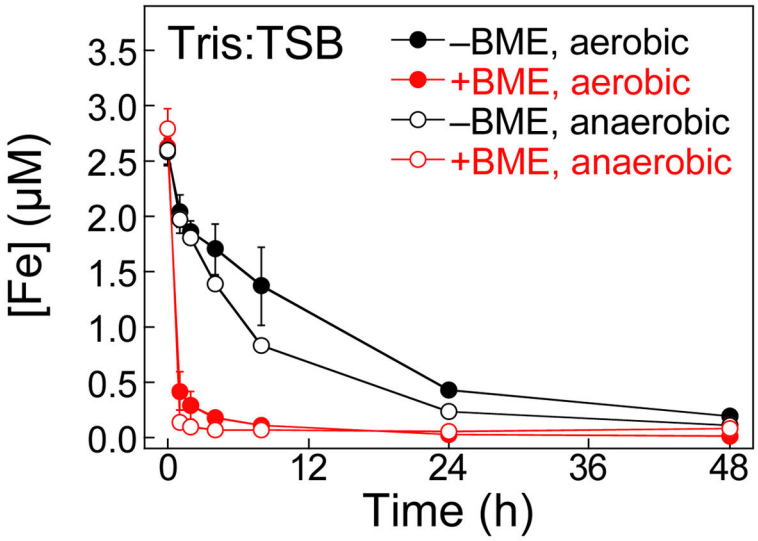

Fig. 3.

Iron depletion by CP-Ser anaerobic conditions. Tris:TSB was treated with 10.5 μM (250 μg/mL) CP-Ser in the absence (black) and presence (red) of ≈3 mM BME under a nitrogen atmosphere at 30 ºC, 150 rpm. The Fe content of the CP-treated medium was analyzed by ICP-MS at t = 0, 1, 2, 4, 8, 24, and 48 h. The mean and SDM are reported (n = 3). The Fe-depletion profiles of CP-Ser under aerobic conditions (±3 mM BME) are reproduced from Fig. 2A.

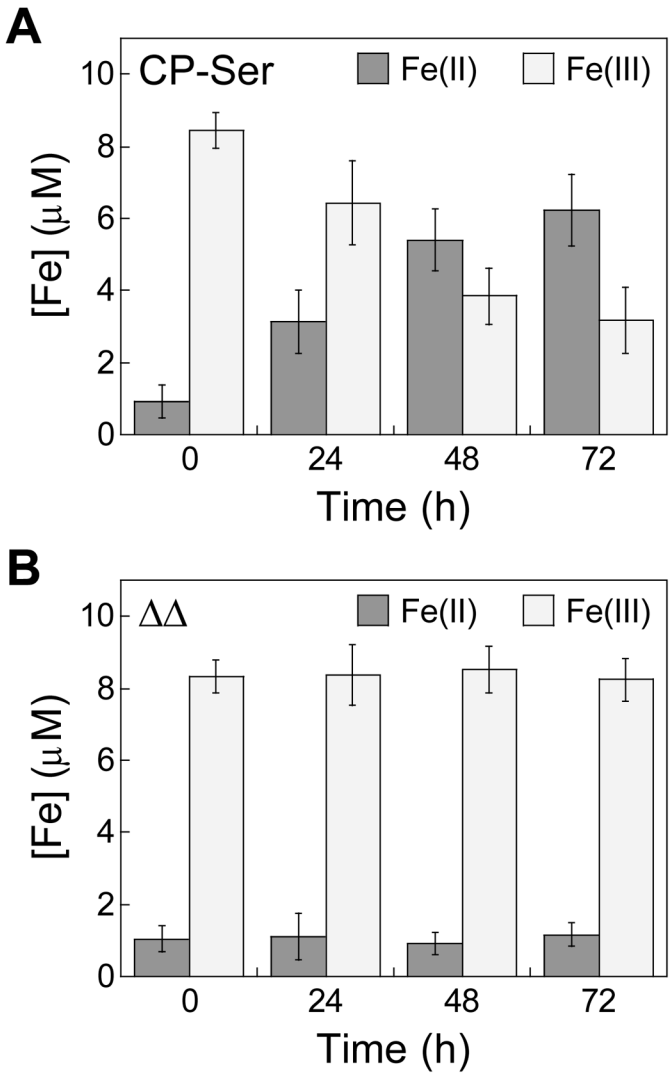

Fig. 4.

CP increases the [Fe(II)]/[Fe(IIII)] ratio in solution. Fe(III) citrate (10 μM) was incubated with 10.5 μM (250 μg/mL) (A) CP-Ser or (B) the ΔΔ in 75 mM HEPES, 100 mM NaCl, 2 mM $CaCl_2$, pH 7.0 at 30 ºC, 150 rpm. The mean and SDM are reported (n = 6).

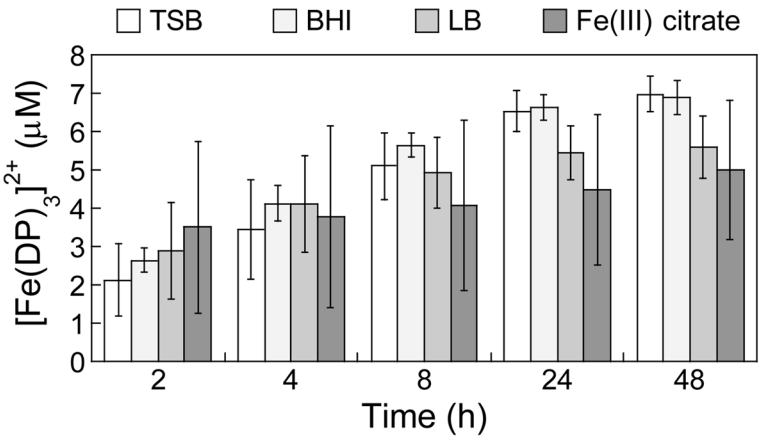

Fig. 5.

Formation of $[Fe(DP)_3]^{2+}$ over time in bacterial growth media (TSB, BHI, LB) and in aqueous buffer (75 mM HEPES, 100 mM NaCl, 2 mM $CaCl_2$, pH 7.0) containing 10 μM Fe(III) citrate and 1 mM DP at 30 °C, 150 rpm. The mean and SDM are reported (n = 6).

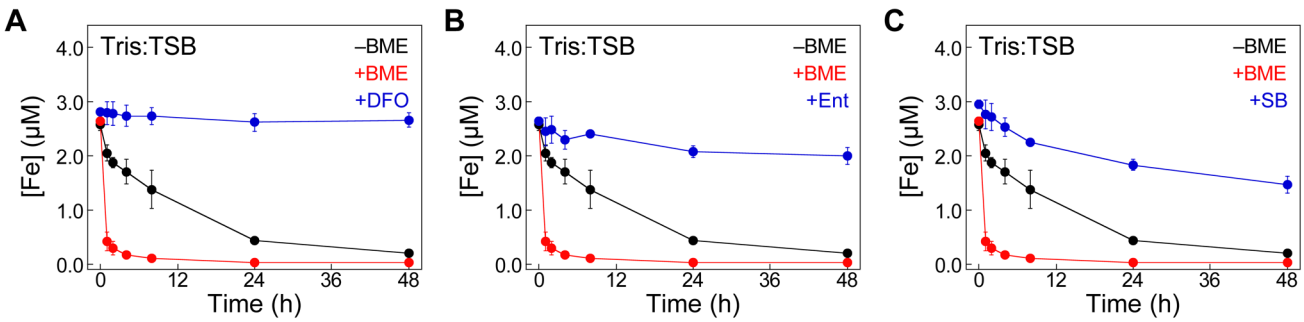

Fig. 6.

The presence of siderophores attenuates Fe depletion by CP. Tris:TSB in the presence of 3 μM (A) DFO, (B) Ent, and (C) SB were treated with 10.5 μM (250 μg/mL) CP-Ser at 30 ºC, 150 rpm. The metal content of the CP-treated medium was analyzed by ICP-MS at t = 0, 1, 2, 4, 8, 24, and 48 h. The mean and SDM are reported (n = 3). The Fe-depletion profiles of CP-Ser in the presence and absence of BME are reproduced from Fig. 2B.

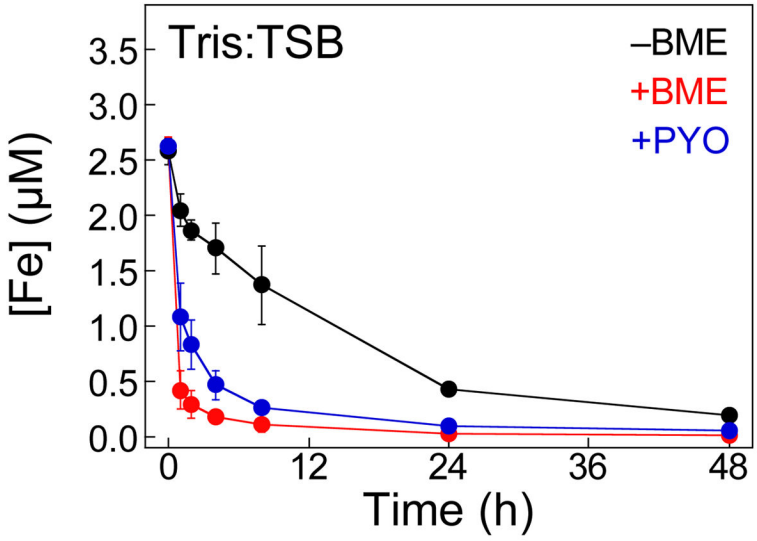

Fig. 7.

The phenazine PYO promotes Fe-depletion by CP-Ser from Tris:TSB under aerobic conditions. The medium was treated with 10.5 μM (250 μg/mL) CP-Ser and10 μM PYO at 30 °C, 150 rpm. The metal content of Fe was analyzed by ICP-MS at t = 0, 1, 2, 4, 8, 24, and 48 h. The mean and SDM are reported (n = 3). The Fe-depletion profiles of CP-Ser in the presence and absence of BME are reproduced from Fig. 2B.